

Supporting Information

Zn(II)-Based Metal-Organic Frameworks with Tailored Architectures: Optimizing Fluorescence Performance for Cell Imaging and Cancer Therapy

Jinglu Wang,^{a#} Yutong Chen,^{b#} Danian Tian,^{*a} Siyi Li,^b Peipei Cen,^{*a} and Xiangyu Liu^b

^a *College of Public Health, Key Laboratory of Environmental Factors and Chronic Disease Control, Ningxia Medical University, Yinchuan 750004, China.*

^b *State Key Laboratory of High-efficiency Utilization of Coal and Green Chemical Engineering, College of Chemistry and Chemical Engineering, Ningxia University, Yinchuan 750021, China.*

[#]These authors contributed equally to this work.

***Corresponding author**

Dr. Peipei Cen

E-mail: 13895400691@163.com

***Corresponding author**

Dr. Danian Tian

E-mail: tiandanian@163.com

Contents

Table S1. Crystallographic data and refinement parameters for compound **1** and **2**.

Table S2. Selected bond lengths (Å) and bond angles (°) for compound **1**.

Table S3. Selected bond lengths (Å) and bond angles (°) for compound **2**.

Figure S1 (a) Coordination environment and geometric configuration of Zn(II) in **1**; (b) The 1D chains of **1**; (c) The 2D layer of **1**; (d) The supramolecular 3D structure of **1**; (e) The π - π Packing diagram of **1** (the dashed line represents the interaction). All hydrogen atoms for **1** are omitted for clarity.

Figure S2 (a) FTIR for DHTA and bix organic ligands; (b) FTIR for **1** and **2** compounds.

Figure S3 PXRD curves of **1** (a) and **2** (b).

Figure S4 TGA curves of **1** and **2**.

Figure S5 The pH stability of **1** (a) and **2** (b).

Figure S6 Solid-state Fluorescence excitation and emission spectra of ligands DHTA (a), bix (b), **1** (c) and **2** (d). (Temperature = 23 °C, $E_{x\text{DHTA}}$ = 425 nm, $E_{x\text{bix}}$ = 440 nm, E_{x1} = 394 nm, E_{x2} = 402 nm.)

Figure S7 Liquid fluorescence pattern of **1** (a) and **2** (b). (The solvent is ultrapure water, pH = 7.0, temperature = 23 °C, E_{x1} = 365 nm, E_{x2} = 370 nm)

Figure S8 The luminescence decay curves of **1** (a) and **2** (b).

Figure S9 Fluorescence intensity of **1** (a) and **2** (b) upon addition of different metal cations (20 μ L) in aqueous solutions. (The solvent is ultrapure water, pH = 7.0, temperature = 23 °C, E_{x1} = 365 nm, E_{x2} = 370 nm)

Figure S10 Fluorescence intensity of **1** (a) and **2** (b) with the addition of different anions (20 μ L) in aqueous solutions. (The solvent is ultrapure water, pH = 7.0, temperature = 23°C, E_{x1} = 365 nm, E_{x2} = 370 nm)

Figure S11 (a) and (b) belong to the transmission electron microscopy image of compound **1** in HeLa cells. Nucleus (N), mitochondria (Mi), rough endoplasmic reticulum (RER), lipid droplets (LD); nuclear shrinkage and widening of perinuclear space (\uparrow), chromatin agglutination (\square), mitochondrial shrinkage (\uparrow), rough endoplasmic reticulum expansion (\uparrow), apoptotic bodies (\uparrow), vacuoles (\uparrow), autophagy (\uparrow).

Figure S12 Energy level diagram of DHTA (a) and bix (b).

Table S1. Crystallographic data and refinement parameters for compound **1** and **2**.

	Compound 1	Compound 2
Empirical formula	C ₂₂ H ₁₈ N ₄ O ₆ Zn	C ₂₂ H ₁₈ N ₄ O ₆ Zn
Formula weight	499.77	499.79
Crystal system	triclinic	monoclinic
Space group	$P\bar{1}$	$C2/c$
$a(\text{\AA})$	8.2605(6)	25.9395 (4)
$b(\text{\AA})$	10.6797(8)	10.8613(2)
$c(\text{\AA})$	13.5264(10)	18.3000(3)
$\alpha(^{\circ})$	106.147(2)	90
$\beta(^{\circ})$	93.965(2)	121.9110(10)
$\gamma(^{\circ})$	102.238(2)	90
$V(\text{\AA}^3)$	1109.69(14)	4376.59(13)
μ (mm ⁻¹)	1.153	1.169
Unique reflections	3894	4482
Observed reflections	25905	22463
R_{int}	0.0513	0.0361
Final R indices [$I > 2 \sigma(I)$]	$R_1 = 0.0546$ $wR_2 = 0.1368$	$R_1 = 0.0350$ $wR_2 = 0.0867$
R indices (all data)	$R_1 = 0.0738$ $wR_2 = 0.1483$	$R_1 = 0.0448$ $wR_2 = 0.0927$

Table S2. Selected bond lengths (Å) and bond angles (°) for compound **1**.

Compound 1			
Zn(1)-O(4)	1.935(3)	O(2)-Zn(1)-N(4 ¹)	118.20(16)
Zn(1)-O(2)	1.979(3)	N(4 ¹)-Zn(1)-N(1)	111.36(16)
Zn(1)-N(4 ¹)	1.995(4)	C(1)-O(4)-Zn(1)	117.6(3)
Zn(1)-N(1)	2.004(4)	C(5)-O(2)-Zn(1)	116.7(3)
O(4)-Zn(1)-O(2)	96.49(14)	C(21)-N(4)-Zn(1 ¹)	124.4(3)
O(4)-Zn(1)-N(4 ¹)	119.39(16)	C(22)-N(4)-Zn(1 ¹)	127.7(3)
O(4)-Zn(1)-N(1)	110.52(16)	C(11)-N(1)-Zn(1)	124.6(3)
O(2)-Zn(1)-N(4 ¹)	100.15(15)	C(9)-N(1)-Zn(1)	129.7(4)

¹1-X, 1-Y, 2-Z; ²2-X, 2-Y, 1-Z; ³2-X, 1-Y, 2-Z

Table S3. Selected bond lengths (Å) and bond angles (°) for compound **2**.

Compound 2			
Zn(1)-O(2)	1.9531(17)	O(4)-Zn(1)-N(1)	103.66(9)
Zn(1)-O(4)	1.9494(17)	N(1)-Zn(1)-N(4 ¹)	108.66(9)
Zn(1)-N(4 ¹)	2.005(2)	C(5)-O(2)-Zn(1)	114.84(16)
Zn(1)-N(1)	1.985(2)	C(1)-O(4)-Zn(1)	117.99(17)
O(2)-Zn(1)-N(4 ¹)	102.31(8)	C(20)-N(4)-Zn(1 ²)	118.60(19)
O(2)-Zn(1)-N(1)	118.22(8)	C(21)-N(4)-Zn(1 ²)	132.8(2)
O(4)-Zn(1)-O(2)	113.50(8)	C(10)-N(1)-Zn(1)	127.18(18)
O(4)-Zn(1)-N(4 ¹)	110.47(8)	C(9)-N(1)-Zn(1)	126.5(2)

¹-1/2+X, -1/2+Y, +Z; ²1/2+X, 1/2+Y, +Z; ³1-X, -Y, 1-Z; ⁴1/2-X, -1/2-Y, -Z

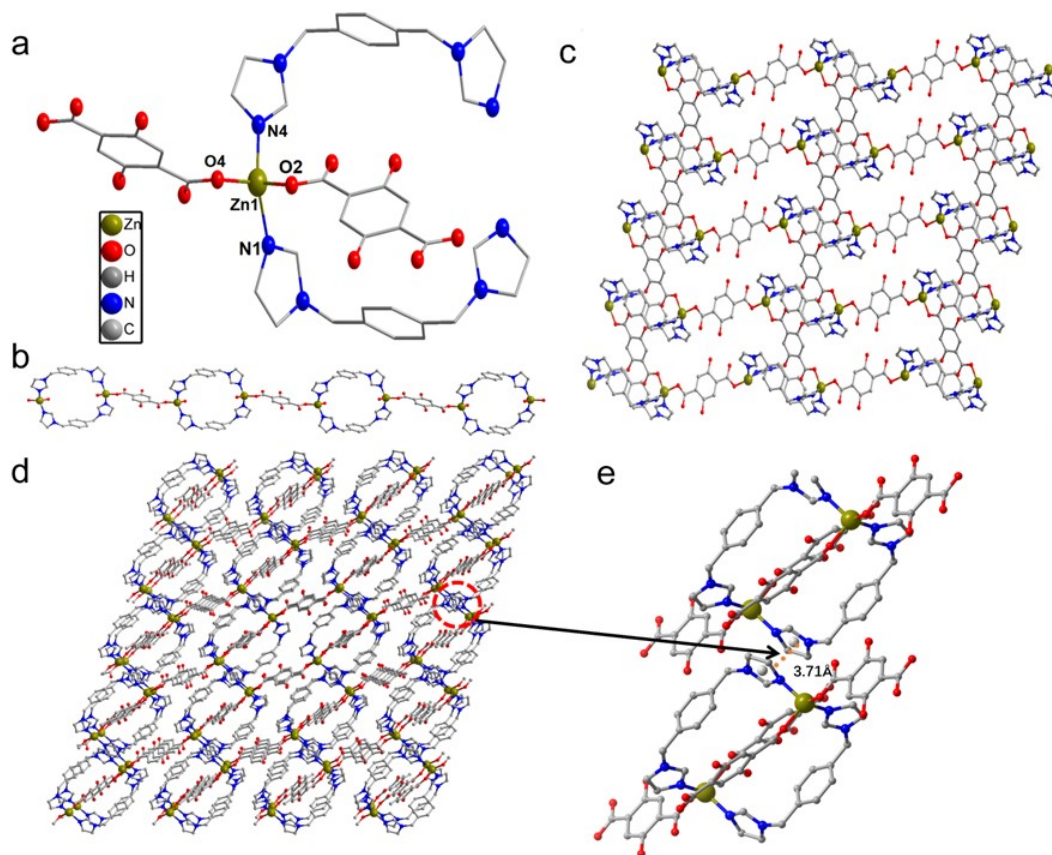


Figure S1 (a) Coordination environment and geometric configuration of Zn(II) in **1**; (b) The 1D chains of **1**; (c) The 2D layer of **1**; (d) The supramolecular 3D structure of **1**; (e) The π - π Packing diagram of **1** (the dashed line represents the interaction). All hydrogen atoms for **1** are omitted for clarity.

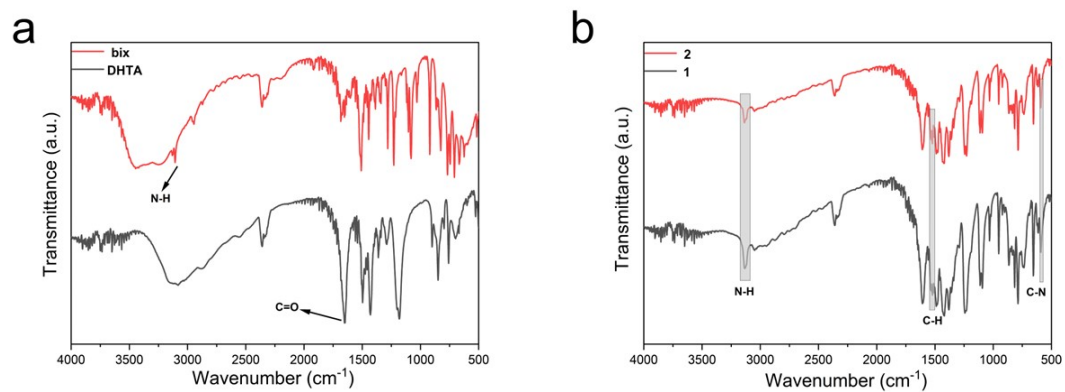


Figure S2 (a) FTIR for DHTA and bix organic ligands; (b) FTIR for **1** and **2** compounds.

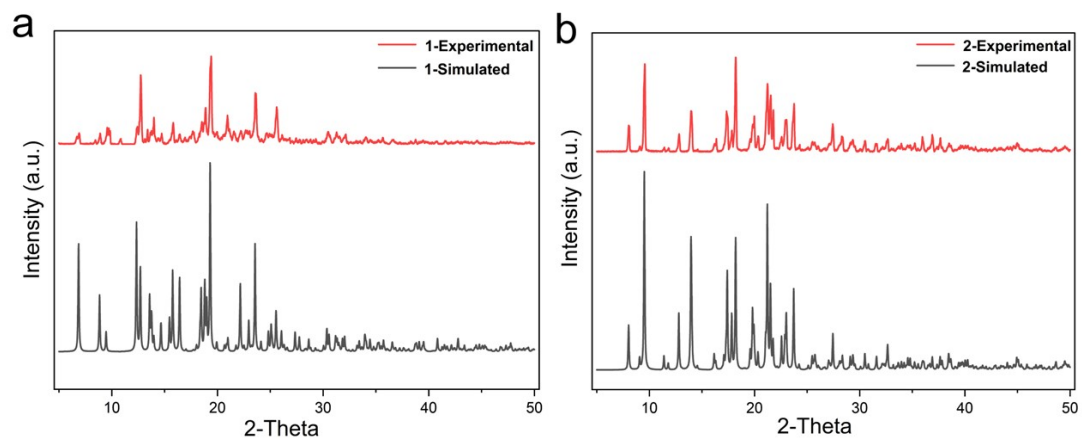


Figure S3 PXRD curves of **1** (a) and **2** (b).

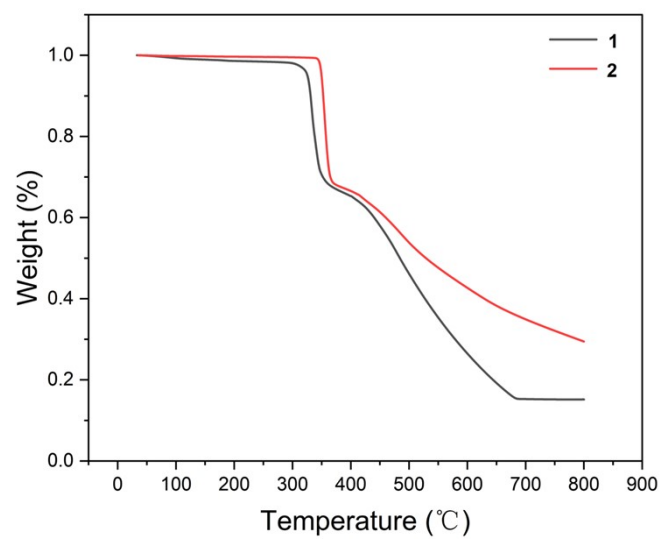


Figure S4 TGA curves of **1** and **2**.

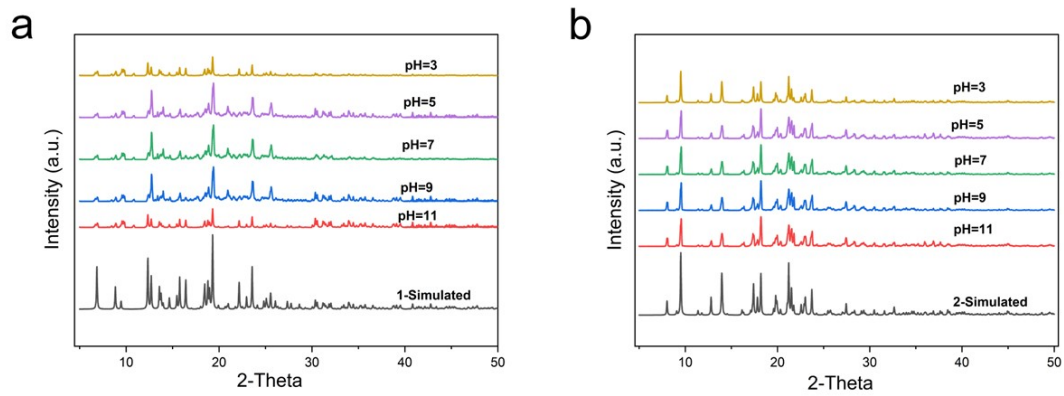


Figure S5 The pH stability of **1** (a) and **2** (b).

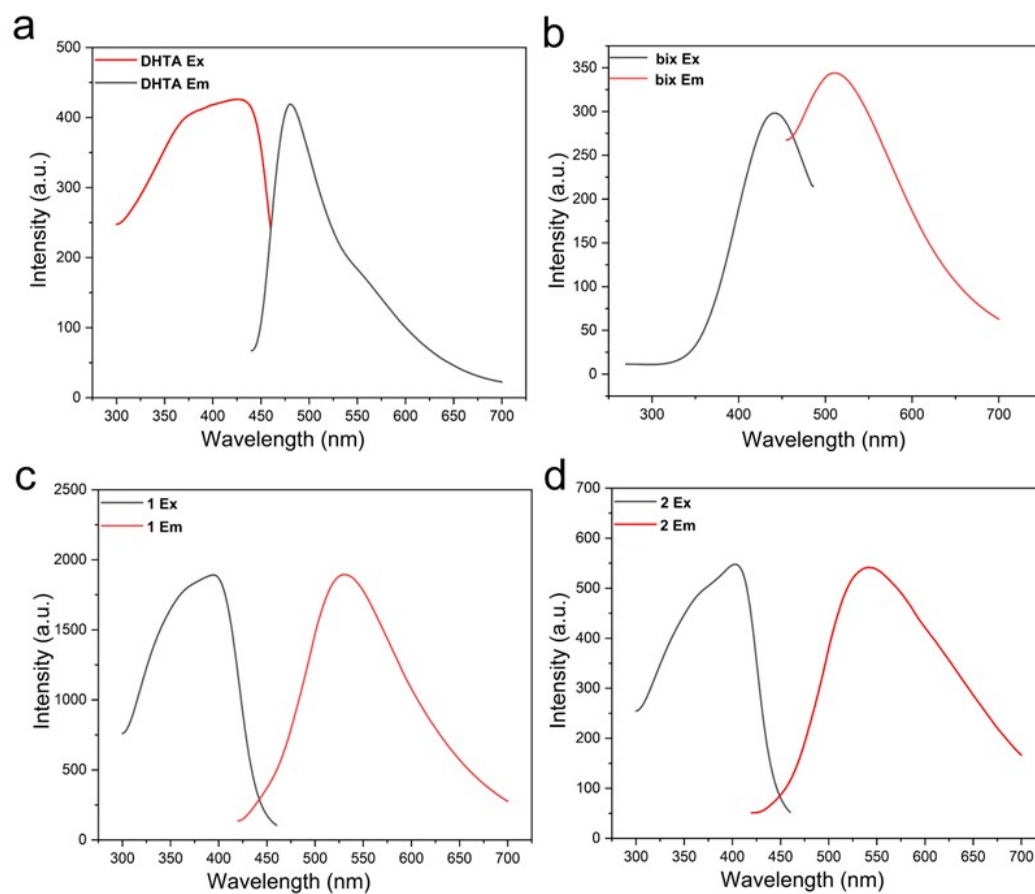


Figure S6 Solid-state Fluorescence excitation and emission spectra of ligands DHTA (a), bix (b), **1** (c) and **2** (d). (Temperature = 23 °C, $E_{x\text{DHTA}} = 425$ nm, $E_{x\text{bix}} = 440$ nm, $E_{x1} = 394$ nm, $E_{x2} = 402$ nm.)

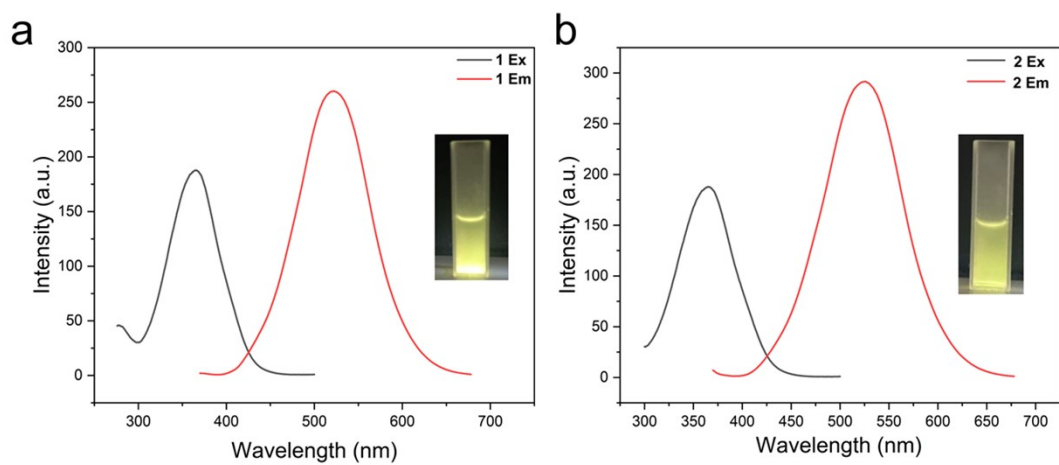


Figure S7 Liquid fluorescence pattern of **1** (a) and **2** (b). (The solvent is ultrapure water, pH = 7.0, temperature = 23 °C, E_{x1} = 365 nm, E_{x2} = 370 nm)

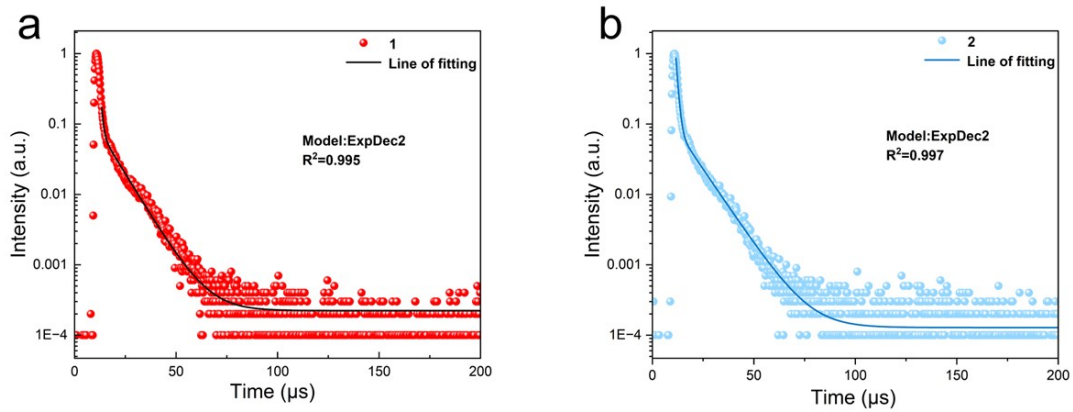


Figure S8 The luminescence decay curves of **1** (a) and **2** (b).

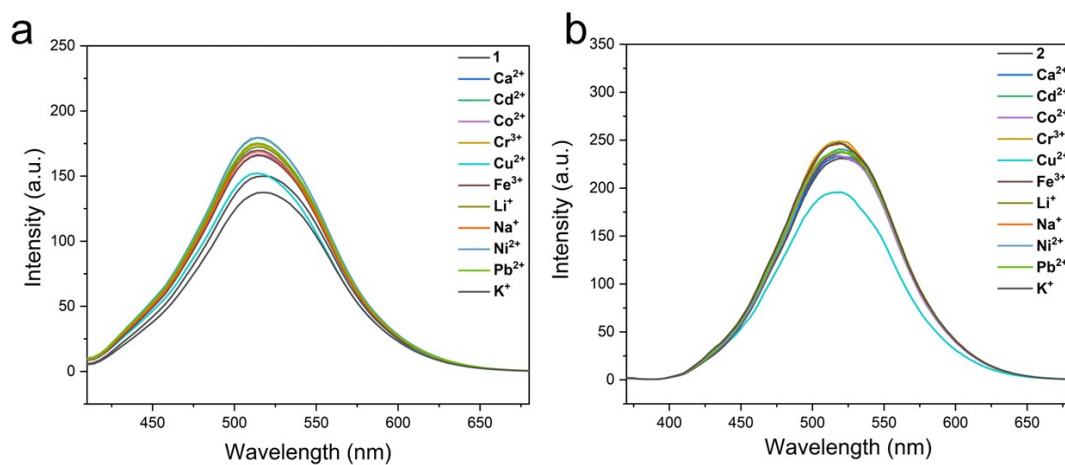


Figure S9 Fluorescence intensity of **1** (a) and **2** (b) upon addition of different metal cations (20 μ L) in aqueous solutions. (The solvent is ultrapure water, pH = 7.0, temperature = 23 $^{\circ}$ C, E_{x1} = 365 nm, E_{x2} = 370 nm)

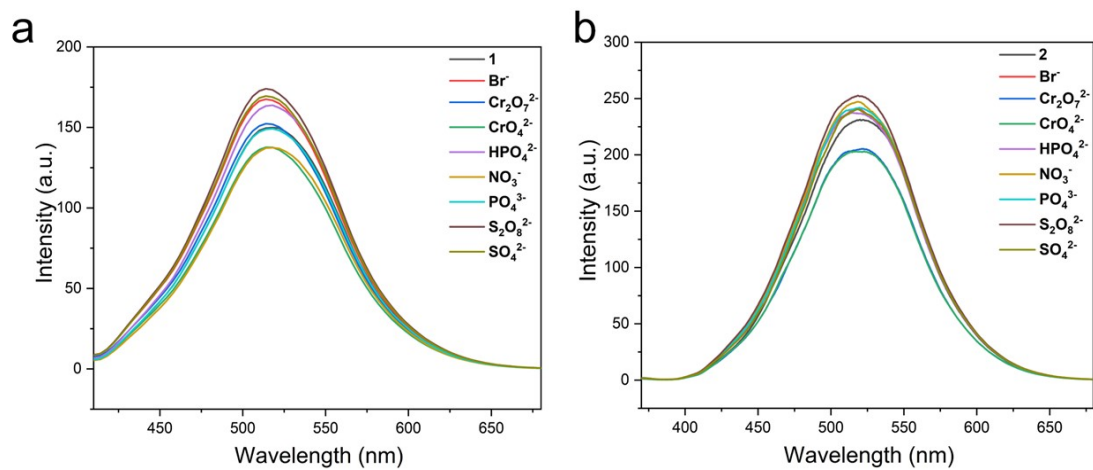


Figure S10 Fluorescence intensity of **1** (a) and **2** (b) with the addition of different anions (20 μL) in aqueous solutions. (The solvent is ultrapure water, $\text{pH} = 7.0$, temperature = 23°C , $E_{x1} = 365 \text{ nm}$, $E_{x2} = 370 \text{ nm}$)

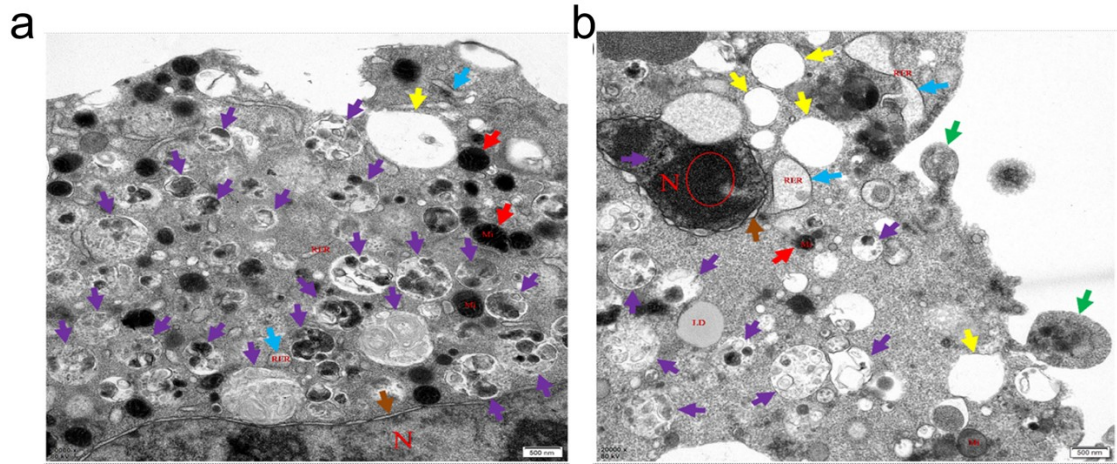


Figure S11 (a) and (b) belong to the transmission electron microscopy image of compound **1** in HeLa cells. Nucleus (N), mitochondria (Mi), rough endoplasmic reticulum (RER), lipid droplets (LD); nuclear shrinkage and widening of perinuclear space (\uparrow), chromatin agglutination (\square), mitochondrial shrinkage (\uparrow), rough endoplasmic reticulum expansion (\uparrow), apoptotic bodies (\uparrow), vacuoles (\uparrow), autophagy (\uparrow).

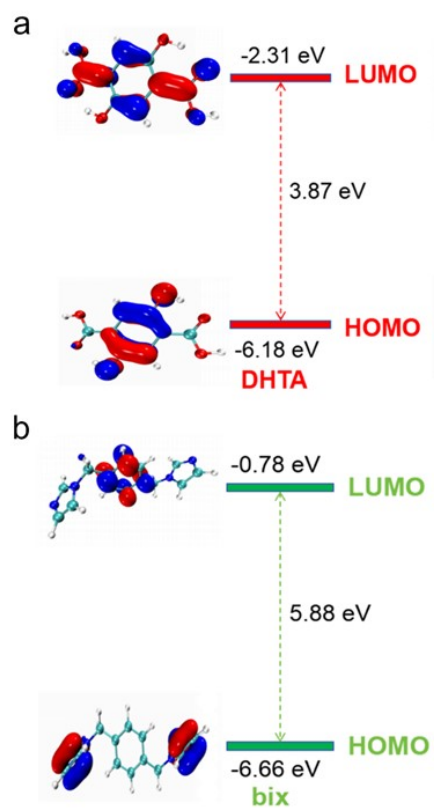


Figure S12 Energy level diagram of DHTA (a) and bix (b).